Analysis of Minimum Cost in Shape-Optimized Litz-Wire Inductor Windings

C. R. Sullivan

J. D. McCurdy

R. A. Jensen

Analysis of Minimum Cost in Shape-Optimized Litz-Wire Inductor Windings

Charles R. Sullivan, Joshua D. McCurdy and Robert A. Jensen

Dartmouth College, Hanover, NH, USA, http://engineering.dartmouth.edu/inductor

Abstract—**Litz-wire windings for gapped inductors are optimized for minimum cost within a loss constraint or vice-versa. Optimal winding shapes and the strand diameter and number for each shape are found through simultaneous consideration of two-dimensional field effects and of cost and ac-loss implications of litz stranding.**

I. Introduction

THE eddy current losses in a gapped inductor depend strongly on the two-dimensional field shape, determined by the gap, the core, and the winding. Conventional one-dimensional analyses of proximity-effect losses [1], [2], [3], [4], [5], [6], [7], [8], [9] do not account for the true field of a gapped inductor, and do not allow accurate prediction of inductor ac resistance [10], [11]. Because of the high flux density near the gap, and the dependence of loss on the square of the field, the loss can be much worse than predicted. One alternative is the modify the structure to introduce a distributed [12], [13] or quasi-distributed gap [14], [15], [16], [17]. However, in [11], [18], it is shown that a simple lumped gap with the winding shape changed to keep the winding away from the gap can result in better performance than an ideal distributed-gap design. Optimal design using this strategy requires an iterative numerical solution, because when the winding shape is changed to keep the winding out of the high-field regions, the field shape changes, and so the location of high-field regions also changes [11].

Although the inductor designs with optimized winding shapes found in [11], [18] represent a significant advance, they depend on some parameters being arbitrarily chosen rather than truly optimized. In [11], the use of litz wire is assumed, and the size of strands in the litz wire must be arbitrarily fixed before the optimization proceeds. In [18], the results of [11] are extended to allow the possibility of arbitrarily fixing the number of strands rather than the diameter of strands. But neither arbitrarily fixing the number of strands nor arbitrarily fixing the diameter of strands corresponds to the real practical design problem. The real reason for not using more or finer strands is a cost constraint, and cost depends on both strand diameter and number of strands. Thus, the designs found in [11], [18] are optimal in only a narrow sense.

The question of optimization of a litz wire winding subject to a cost constraint has been addressed in [19], [20], where it is shown that considering cost can lead to significant cost and/or loss savings. However, the results in [19] are limited to simple geometries with one-dimensional fields. Because considering cost is essential to selecting a good design, the analysis in [19] has been applied to gapped inductors, despite the inaccuracy in that approach [21]. In this paper, we show how to accurately analyze the cost/loss tradeoff in a litz wire winding for a gapped inductor through minimization of loss subject to a cost constraint, using the two-dimensional loss analysis and shape optimization developed in [11], [18] in conjunction with the cost model proposed in [19].

II. Optimized-Shape Windings

The numerical optimization in [11] results in the winding shapes shown in Fig. 1 for 0.1 mm litz strand diameter and a 10 mm square winding window. The analysis in [11], [18] and the analysis below are two-dimensional and neglect the effects of curvature or different winding lengths at different positions in the window.

Each one of the shapes such as those in Fig. 1 is not only optimal for the specific conditions of frequency and strand diameter for which it was chosen, but it is also the shape that, given a particular amount of area for the winding, minimizes the exposure of the winding to the field. Thus, for any parameters in that window geometry, the set of optimal shapes will be the same, but which one is best for a given frequency may vary.

In order to minimize loss for a given cost, we will use one of the shapes in Fig. 1, or an interpolation between them. (For different core window shapes, new sets of winding optimizations are needed.) The choice of number of litz wire strands and diameter of those strands determines the area necessary (for a given number of turns) and so determines which shape is required. We then need expressions for both loss and cost in order to perform an optimization.

III. Models used

A. Loss calculation

The calculation of loss, given a choice of strand diameter and number of strands follows that in [11], [18]. For cylindrical conductors with diameter, d, small compared to a skin depth, the eddy-current (proximity-effect) loss in a sinusoidal ac field of amplitude B, perpendicular to the axis of the wire, at a frequency ω is [8],

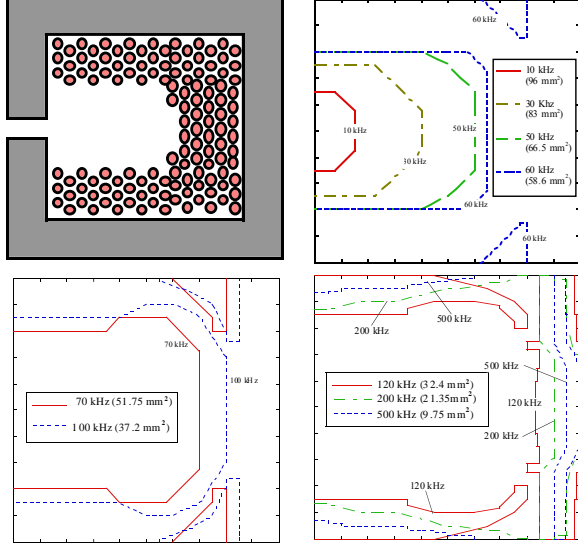$$P_e = \frac{\pi \omega |B|^2 \ell d^4}{128 \cdot \rho_c} \qquad (1)$$

Fig. 1. Optimized winding shapes, from [11]. Upper left is a drawing corresponding approximately to the optimized shape for 50 kHz with a square 10 mm winding window and litz wire with 0.1 mm stand diameter. The remaining three figures show the shapes obtained for a range of frequencies. For other strand diameters or frequencies, the set of shapes will be same, but the frequency correspondence will differ.

where ℓ is the length of the conductor and ρ_c is the resistivity of the conductor. For nonsinusoidal waveforms, an "effective frequency" [22], [23], [24], [25] may be substituted for ω, allowing the analysis below to apply directly (Appendix A).

For the complete winding,

$$P_e = \frac{\pi \omega^2 F_p}{128 \rho_c} \ell_t d^2 \int_{A_u} |B|^2 \cdot dA = \frac{\pi \omega^2 F_p}{128 \rho_c} \ell_t d^2 A_u \overline{|B|^2} \quad (2)$$

where ℓ_t is the length of a turn, A_u is the portion of the window area that is actually used, $\overline{|B|^2}$ is the spatial average of the squared field magnitude in that region, and F_p is the winding packing factor relative to ideal square packing $F_p = \frac{nN\pi d^2}{4A_u}$, with N the number of turns and n the number of strands per turn. From (2) one can see that the proximity effect loss is proportional to the area times the average value of the square of the flux density, $A_u \overline{|B|^2}$. The resistive loss, however, is inversely proportional to A_u

$$P_r = \frac{4 I_{total}^2 \rho_c \ell_t}{\pi F_p A_u}, \quad (3)$$

where total winding current is defined as $I_{total} \equiv NI$.

To evaluate the tradeoff between eddy and resistive loss, we need to consider not only the effect of area used, A_u, on loss, but also the effect of A_u on $\overline{|B|^2}$. This latter relationship depends only on the core geometry and winding shape, and not on details such as winding current or number of turns, if we
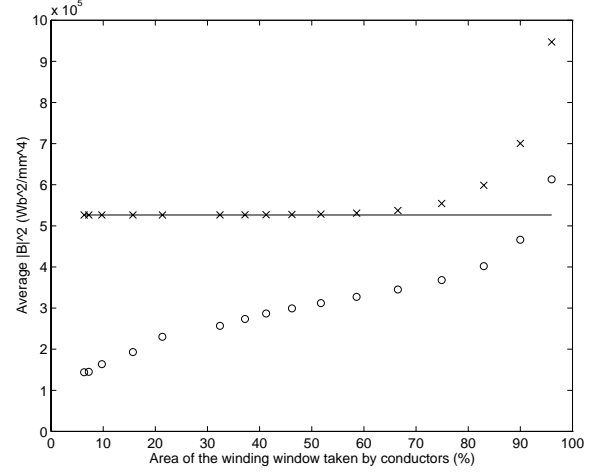

Fig. 2. Relationship between $\overline{|B|^2}$ and window area used (o). Also shown is the value of $\overline{|B|^2}$ with non-optimized rectangular winding shapes (x) and the value of $\overline{|B|^2}$ calculated based on one-dimensional analysis (solid line).

normalize $\overline{|B|^2}$ to the total winding current $NI = I_{total}$. We define this normalized function as

$$g(A_u) = \frac{\overline{|B|^2}}{I_{total}^2}. \quad (4)$$

This function may be found from one set of numerical optimization data, such as that shown in Fig. 1, and is shown in Fig. 2.

Total winding loss may be found by summing eddy loss (2) and resistive loss (3):

$$P_w = \frac{k_r}{A_u} + k_e d^2 g(A_u) A_u \quad (5)$$

where k_r is a resistive loss constant

$$k_r \equiv \frac{4 I_{total}^2 \rho_c \ell_t}{\pi F_p} \quad (6)$$

and k_e is an eddy-current loss constant

$$k_e \equiv \frac{\pi \omega^2 F_p \ell_t I_{tot}^2}{128 \rho_c}. \quad (7)$$

B. Cost Model

Attempting to quantify cost for academic analysis is problematic; prices change with volume, manufacturer, time, and negotiation. However, many important results depend only on the general form of the cost function. In particular, the general solution developed here for optimal cost/loss tradeoff designs depends only on the assumption that the cost of a length of litz wire can be approximately described by [19]
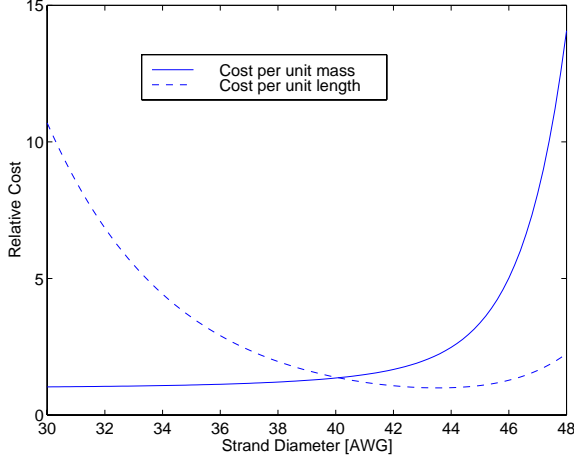
$$Cost = (C_0 + C_m(d)d^2 n)\ell \quad (8)$$

Fig. 3. Normalized cost per unit mass and normalized cost per unit length, as modeled by (9) Both are normalized such that the minimum values are one, for the purpose of display in this graph. The cost per unit mass increases monotonically, reflecting the cost of drawing a given quantity of copper into finer and finer strands.

where C_0 is a base cost per unit length associated with the bundling and serving operations, $C_m(d)$ is a cost basis function proportional to the additional cost per unit mass for a given strand diameter d, n is the number of strands, and ℓ is the length of the wire. Note that for the purpose of optimization with a fixed winding length, we can ignore C_0, and consider only the cost variation which is proportional to $C_m(d)d^2n$.

In [19], an approximate expression for a normalized $C_m(d)$ is also found, via a curve fit to manufacturers' pricing

$$C_m(d) = 1 + \frac{k_1}{d^6} + \frac{k_2}{d^2} \qquad (9)$$

where d is in meters, $k_1 = 1.1 \times 10^{-26}$ m^6, and $k_2 = 2 \times 10^{-9}$ m^2. This function, proportional to cost per unit mass, is shown in Fig. 3, along with the normalized cost per unit length, $C_m(d)d^2$.

IV. OPTIMIZATION

All the necessary analyses are now in place to determine the minimum-loss choice of number and diameter of strands for a given cost. The choice of holding cost fixed and minimizing loss is only for convenience; the set of these choices for different costs will also be the set of minimum cost designs for various given losses.

Using the cost model discussed in Section III-B, we can express total cost as

$$C_{tot} = C_m(d)\ell_t N d^2 n = \ell_t N C_m(d) k_p A_u \qquad (10)$$

where k_p is an overall packing constant defined as

$$k_p \equiv \frac{nd^2}{A_u} = \frac{4F_p}{N\pi}. \qquad (11)$$

To minimize loss with fixed cost we fix C_{tot}. Since N and ℓ_t are also fixed, we can factor them out and fix a newly defined normalized cost variable

$$C_{tn} \equiv \frac{C_{tot}}{\ell_t N} = C_m(d)d^2n = C_m(d)k_p A_u. \qquad (12)$$

With the cost fixed, we can substitute $n = \frac{C_{tn}}{Cm(d)d^2}$ into (5), and, also substituting $A_u = \frac{nd^2}{k_p}$, this results in

$$P_w = \frac{k_r k_p C_m(d)}{C_{tn}} + \frac{k_e C_{tn}}{k_p C_m(d)}d^2 g\left(\frac{C_{tn}}{K_p C_m(d)}\right) \qquad (13)$$

The optimum value of d for the fixed cost can be obtained by differentiating this expression with respect to d and setting the result equal to zero,

$$\frac{k_r k_p^2 C_m'(d)C_m(d)}{k_e C_{tn}^2} + \left[2 - \frac{C_m'(d)}{C_m(d)}d\right] dg\left(\frac{C_{tn}}{K_p C_m(d)}\right)$$
$$- \frac{C_m'(d)C_{tn}}{C_m^2(d)k_p}d^2 g'\left(\frac{C_{tn}}{K_p C_m(d)}\right) = 0, \quad (14)$$

where $g'(\cdot)$ and $C_m'(\cdot)$ are the derivatives of those functions with respect to their arguments. Without a closed-form expression for $g(A_u)$, this expression must be solved numerically for the optimum d to obtain minimum loss for a given cost. In practice, it may be desirable to find the lowest cost for a given loss instead, or to obtain a plot of the full range of possibilities from which the best choice for a given circuit may be chosen. Thus, it is useful to eliminate C_{tn} from (14)
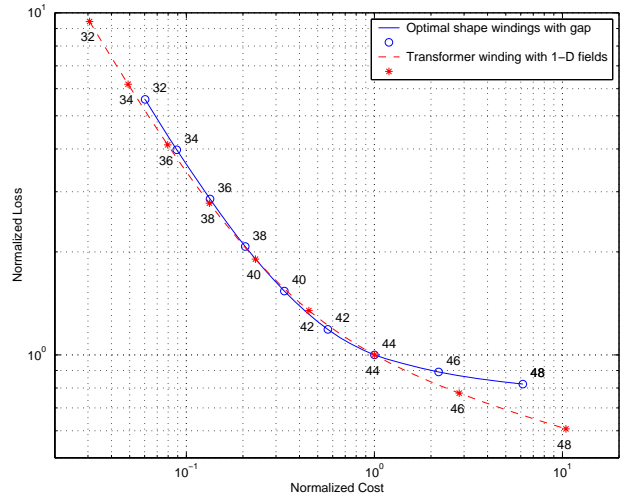

Fig. 4. The cost and loss of a range of possible designs (solid line) for optimal cost/loss tradeoff in a gapped inductor with an optimized winding shape. AWG stand sizes required to achieve the plotted points are indicated. This particular curve is for a 10 mm square winding window and a 50 kHz operating frequency; the curve varies slightly for different frequencies and also varies for other winding window sizes and aspect ratios. The dotted line shows the same tradeoff for a simple one-dimensional case.

using (12) to obtain (after some rearrangement)

$$\left[\frac{k_r}{k_e A_u^2} - \frac{k_p}{N} A_u^2 g'(A_u) \right] \frac{1}{g(A_u)} = d^2 - 2\frac{C_m(d)}{C_m'(d)}d. \quad (15)$$

This is a relationship between the area of the bobbin used A_u and the strand diameter. For the curve of design options it describes, one may calculate the cost and loss from (10) and (5). These are plotted, normalized, in Fig. 4. For comparison, the corresponding normalized cost/loss curve for a case with one-dimensional fields [19] is plotted on the same axes. The curves are very similar, but for fine strands, the slope of the curve for the optimized-winding-shape gapped inductor is lower, indicating that the loss improves relatively slowly as more money is spent on larger numbers of finer litz strands, compared to the one-dimensional case. This is explained by the fact that the more expensive designs use a larger area of the winding window, and thus the average value of the field to which the winding is exposed increases, as reflected in the function $g(A_u)$ (Fig. 2). This partially offsets the gains from the use of more strands of finer wire, and so the possible improvement from a given investment in wire is not a great as it would be with a flat $g(A_u)$, as in the one-dimensional case.

In the one-dimensional case, the cost/loss curves for any two different designs with different parameters (window geometry, frequency, etc.) are identical if they are both normalized to the cost and loss of the same strand size [19]. Unfortunately, with two-dimensional field and winding geometries, the curves are no longer identical, although they remain similar. The curve in Fig. 4 shows but one particular example. Equation (15) must be solved for each new set of parameters.

Fig. 5 shows, for example, the results for the same parameters as in Fig. 4, but for twice the frequency. The curve is generally similar, but is not as flat in the fine wire region; it is more similar to the curve for one-dimensional fields. Fig. 5 also shows the full range of possible non-optimal designs for each even AWG strand size. This allows comparing the designs that give minimum loss for a given strand diameter, as would be calculated directly from the analysis in [11], to the optimal cost/loss designs derived here. The results of the simple optimization based on fixed strand size [11] would be the minimum "valley" in each strand-size curve. For fine strands, these minima are very close to the optimal cost/loss curve. Thus, in practice, for fine-strand designs, it may be sufficient to perform only the optimization for a fixed strand diameter as in [11], and directly use those results. However, in the case of larger strands, Fig. 5 shows that the optimal cost-loss designs offer improvements in the range of 20% in cost or loss compared to the designs of minimum loss for a given strand diameter.

To select a particular design from the options found by our analysis and shown in, for example, Fig. 4, one could minimize total cost including the cost of the energy dissipated over the life of the equipment, and other costs that indirectly result from lower efficiency and higher heat production. An example including the cost of energy is discussed in [19].

A. Optimal ac resistance factor

It is elucidative to also express the results in terms of the optimal ac resistance factor $F_r = \frac{R_{ac}}{R_{dc}}$. Appendix B details the calculation of the following expression for the optimal cost/loss value of ac resistance factor:

$$F_{r,CL} = 1 + \frac{1}{1 - 2\frac{C_m(d)}{C_m'(d)d} + \frac{g'(A_u)}{g(A_u)}A_u} \quad (16)$$

This result is consistent with previous results in the literature, including, for a fixed strand diameter in an optimal winding shape [18],

$$F_{r,opt} = 1 + \frac{1}{1 + \frac{g'(A_u)}{g(A_u)}A_u} \quad (17)$$

and for a one-dimensional field with full consideration of cost as a function of number and diameter of strands [19],

$$F_{r,CL} = 1 + \frac{1}{1 - 2\frac{C_m(d)}{C_m'(d)d}}. \quad (18)$$

The consistency between (16) and the previous results (17),(18) can be seen by first considering a cost function that is constant until it increases abruptly above a fixed diameter, effectively constraining the design to that diameter. With $C_m'(d)$ infinite, (16) reduces to (17). With a one-dimensional field, $g(A_u)$ is constant, and (16) reduces to (18).
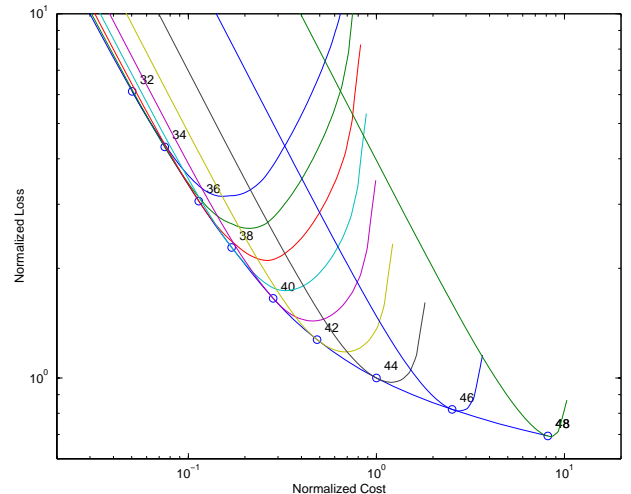

Fig. 5. The cost and loss of designs with optimal cost/loss tradeoff in a gapped inductor with an optimized winding shape, plotted with the full range of possible non-optimal designs for each even AWG strand size. This particular curve is for a 10 mm square winding window and a 100 kHz operating frequency; the curve varies slightly for different frequencies and also varies for other winding window sizes and aspect ratios.
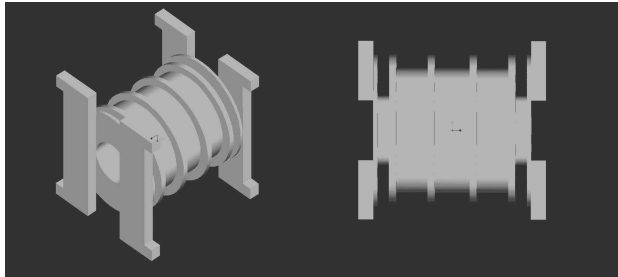
Fig. 6.   Two views of a bobbin for optimized-shape winding, for an EC70 ferrite core. Overall length is about 70 mm.

Fig. 7. Experimental inductor.

Another familiar previous result is that the optimal ac resistance factor is equal to 1.5 for a fixed number of strands (usually one). This is also special case of (18), if we choose the appropriate cost function, $C_m(d)$, that makes the cost independent of diameter, depending only on the number of strands. Since the total cost is proportional to $C_m(d)nd^2$, choosing $C_m(d) \propto \frac{1}{d^2}$ will give total cost independent of diameter, depending only on the number of strands. Substituting this into (18) gives the familiar result of $F_{r,opt} = 1.5$, again confirming consistency of the present work with established results.

V. EXAMPLE DESIGN AND EXPERIMENTAL RESULTS

A 19 mH inductor for a 100 kHz, 0.5 A rms sine wave current in a resonant converter was designed using AWG 46 strand litz wire and optimal winding shape. As shown in Fig. 5, at AWG 46 the minimum loss design for a given strand diameter is very close to the optimum cost/loss frontier, and so we simply selected the minimum loss design using AWG 46 rather than explicitly calculating the cost/loss tradeoff. The first design targeted 10 W total loss (winding and core) on an EC70 core. 10 W of loss represents 0.3 % of the 3300 VA handled by the inductor, and corresponds to an ESR of 40 Ω and a Q of three hundred.

A close approximation to this design was built, using different wire based on what was available from stock. To construct the optimized-shape winding, custom bobbins (Fig. 6) were fabricated with a fusion-deposition-molding rapid-prototyping machine. The experimental inductor is shown in Fig. 7. Low-signal measurements were performed in resonance with an air capacitor, which could be assumed lossless. The ESR was measured as 39 Ω, close to the original predicted ESR. However, in the process of analyzing differences between the original loss predictions and the design based on stock materials, we found an error in the original design calculations, such that the original design was actually far from optimal, and missed substantial opportunities for loss reduction. A newly calculated design is predicted to have approximately half the loss of the original (5 W), but requires a new bobbin shape using more of the winding window. It has not yet been constructed.
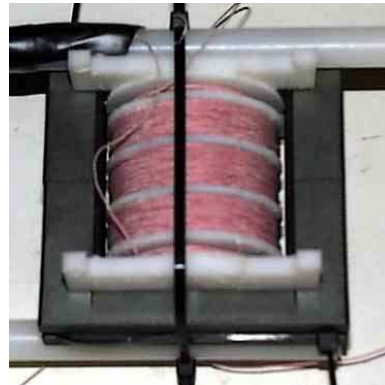
VI. CONCLUSIONS

For the first time, a rigorous gapped-inductor winding optimization has been developed simultaneously considering wire costs and two-dimensional field effects. The results allow a designer to choose between higher-cost, lower-loss designs and lower-cost, higher-loss designs after seeing the full range of possibilities, each of which provides the minimum loss for different given cost (and the minimum cost for a given loss). The results are shown to be consistent with previous results in the literature.

There remain at least two important limitations of the present analysis. It neglects the effects of curvature of the winding. In particular, the length of any turn is assumed to be equal to a fixed average turn length. The optimized designs with wire crowded far from the gap tend to increase average turn length and thus increase resistance in a manner that is not yet accounted for in our analysis. A second limitation is that there are still parameters that are assumed fixed and are not optimized, such as the core size and geometry and number of turns. However, after a core and number of turns are chosen by conventional design methods, the approach here can provide a low-loss winding with minimal cost.

APPENDIX

I. EFFECTIVE FREQUENCY FOR NON-SINUSOIDAL CURRENT WAVEFORMS

Although calculations of winding loss with non-sinusoidal waveforms may be performed using Fourier analysis, the use of an "effective frequency" can allow the analysis above to be used directly. This and similar approaches have been discussed in [22], [23], [24], [25]. Here, we summarize the conclusions on this issue from [24].

For situations in which the frequency-dependent component of loss is proportional to frequency squared, as in (1), an effective frequency that will give the same loss as a component-

by-component Fourier analysis is given by

$$\omega_{eff} = \sqrt{\frac{\sum_{j=0}^{\infty} I_j^2 \omega_j^2}{\sum_{j=0}^{\infty} I_j^2}}. \tag{19}$$

where I_j is the rms amplitude of the Fourier component at frequency ω_j. It is often easier to use the equivalent expression

$$\omega_{eff} = \frac{RMS\{\frac{d}{dt}i(t)\}}{I_{tot,rms}}. \tag{20}$$

The necessary rms values for many common waveforms are tabulated in [25]. It is apparent that (20) is not bounded for waveforms such as square waves with infinite-slope edges. However, practical current waveforms have bounded slopes, especially in inductors.

II. DERIVATION OF AC RESISTANCE FACTOR

The ac resistance factor $F_r = \frac{R_{ac}}{R_{dc}}$ can also be expressed as $F_r = 1 + \frac{P_e}{P_r}$, where P_e is eddy current (or "ac") loss and $P_r = I_{rms}^2 R_{dc}$ is loss due to dc resistance. Using this latter form and expressing P_e and P_r as in the two terms of (5), we can express ac resistance factor as

$$F_r = 1 + \frac{k_e d^2 g(A_u) A_u}{\frac{k_r}{A_u}} \tag{21}$$

To find F_r for optimal cost-loss designs, we first rearrange (15) as

$$\frac{k_r}{k_e A_u^2 g(A_u) d^2} = \frac{k_p A_u^2 g'(A_u)}{N d^2 g(A_u)} + 1 - 2 \frac{C_m(d)}{C'_m(d) d}. \tag{22}$$

The left-hand-side of (22) is the inverse of the fraction in (21). Thus, (21) can be re-written using the right-hand-side of (22) as:

$$F_{r,CL} = 1 + \frac{1}{\frac{k_p A_u^2 g'(A_u)}{N d^2 g(A_u)} + 1 - 2 \frac{C_m(d)}{C'_m(d) d}}. \tag{23}$$

From the definition of k_p (11), $k_p A_u / N = d^2$, and so (23) can also be written as

$$F_{r,CL} = 1 + \frac{1}{1 - 2 \frac{C_m(d)}{C'_m(d) d} + \frac{g'(A_u)}{g(A_u)} A_u}. \tag{24}$$

REFERENCES

[1] P.L. Dowell, "Effects of eddy currents in transformer windings", *Proceedings of the IEE*, vol. 113, no. 8, pp. 1387–1394, Aug. 1966.

[2] J. A. Ferreira, "Improved analytical modeling of conductive losses in magnetic components", *IEEE Transactions on Power Electronics*, vol. 9, no. 1, pp. 127–31, Jan. 1994.

[3] J. Jongsma, "Minimum loss transformer windings for ultrasonic frequencies, part 1: Background and theory", *Phillips Electronics Applications Bulletin*, vol. E.A.B. 35, no. 3, pp. 146–163, 1978.

[4] J. Jongsma, "Minimum loss transformer windings for ultrasonic frequencies, part 2: Transformer winding design", *Phillips Electronics Applications Bulletin*, vol. E.A.B. 35, no. 4, pp. 211–226, 1978.

[5] P. S. Venkatraman, "Winding eddy current losses in switch mode power transformers due to rectangular wave currents", in *Proceedings of Powercon 11*. Power Concepts, Inc., 1984, pp. 1–11.

[6] N. R. Coonrod, "Transformer computer design aid for higher frequency switching power supplies", in *IEEE Power Electronics Specialists Conference Record*, 1984, pp. 257–267.

[7] J. P. Vandelac and P. Ziogas, "A novel approach for minimizing high frequency transformer copper losses", in *IEEE Power Electronics Specialists Conference Record*, 1987, pp. 355–367.

[8] E. C. Snelling, *Soft Ferrites, Properties and Applications*, Butterworths, second edition, 1988.

[9] Audrey M. Urling, Van A. Niemela, Glenn R. Skutt, and Thomas G. Wilson, "Characterizing high-frequency effects in transformer windings–a guide to several significant articles", in *APEC 89*, Mar. 1989, pp. 373–385.

[10] Rudy Severns, "Additional losses in high frequency magnetics due to non ideal field distributions", in *APEC '92. Seventh Annual IEEE Applied Power Electronics Conference*, 1992, pp. 333–8.

[11] Jiankun Hu and Charles R. Sullivan, "Optimization of shapes for round-wire high-frequency gapped-inductor windings", in *Proceedings of the 1998 IEEE Industry Applications Society Annual Meeting*, 1998, pp. 900–906.

[12] Khai D. T. Ngo and M. H. Kuo, "Effects of air gaps on winding loss in high-frequency planar magnetics", in *PESC88*, 1988, pp. 1112–19.

[13] W. M. Chew and P. D. Evans, "High frequency inductor design concepts", in *22nd Annual IEEE Power Electronics Specialists Conference*, June 1991, vol. 22, pp. 673–678.

[14] U. Kirchenberger, M. Marx, and D. Schroder, "A contribution to the design optimization of resonant inductors in high power resonant converters", in *IEEE Industry Applications Society Annual Meeting*, 1992, vol. 1, pp. 994–1001.

[15] W. A. Roshen, R. L. Steigerwald, R. J. Charles, W. G. Earls, G. S. Claydon, and C. F. Saj, "High-efficiency, high-density MHz magnetic components for low profile converters", *IEEE Transaction on Industry Applications*, vol. 31, no. 4, pp. 869–78, 1995.

[16] Jiankun Hu and C. R. Sullivan, "The quasi-distributed gap technique for planar inductors: Design guidelines", in *Proceedings of the 1997 IEEE Industry Applications Society Annual Meeting*, 1997, pp. 1147–1152.

[17] N. H. Kutkut and D. M. Divan, "Optimal air-gap design in high-frequency foil windings", *IEEE Transactions on Power Electronics*, vol. 13, no. 5, pp. 942–9, 1998.

[18] Jiankun Hu and Charles R. Sullivan, "Analytical method for generalization of numerically optimized inductor winding shapes", in *30th Annual IEEE Power Electronics Specialists Conference*, 1999, vol. 1, pp. 568–73.

[19] Charles R. Sullivan, "Cost-constrained selection of strand wire and number in a litz-wire transformer winding", *IEEE Transactions on Power Electronics*, vol. 16, no. 2, pp. 281–288, Mar. 2001.

[20] Charles R. Sullivan, "Cost-constrained selection of strand wire and number in a litz-wire transformer winding", in *Proceedings of the 1998 IEEE Industry Applications Society Annual Meeting*, 1998, pp. 907–911.

[21] A. M. Tuckey and D. J. Patterson, "A minimum loss inductor design for an actively clamped resonant dc link inverter", in *Proceedings of the 1999 IEEE Industry Applications Society Annual Meeting*, 1999, pp. 3119–26.

[22] P. N. Murgatroyd, "The toroidal cage coil", *IEE Proceedings, Part B*, vol. 127, no. 4, pp. 207–214, 1980.

[23] Sergio Crepaz, "Eddy-current losses in rectifier transformers", *IEEE Transactions on Power Apparatus and Systems*, vol. PAS-89, no. 7, pp. 1651–1662, 1970.

[24] Charles R. Sullivan, "Optimal choice for number of strands in a litz-wire transformer winding", *IEEE Transactions on Power Electronics*, vol. 14, no. 2, pp. 283–291, 1999.

[25] W.G. Hurley, E. Gath, and J.G. Breslin, "Optimizing the ac resistance of multilayer transformer windings with arbitrary current waveforms", *IEEE Transactions on Power Electronics*, vol. 15, no. 2, pp. 369–76, Mar. 2000.